The Laryngoscope
Lippincott Williams & Wilkins, Inc.

Temporal Bone Imaging in *GJB2* Deafness

Evan J. Propst, MSc, MD; Susan Blaser, MD, FRCPC; Tracy L. Stockley, PhD;
Robert V. Harrison, PhD, DSc; Karen A. Gordon, MA, PhD; Blake C. Papsin, MSc, MD, FRCSC

Objective: **To describe temporal bone findings on computed tomography (CT) imaging in *GJB2*-related hearing loss (HL). We asked whether evaluation of the temporal bone is required in individuals with biallelic *GJB2* mutations.** ***Study Design:*** **Randomized, blinded, controlled, prospective measurement.** ***Methods:*** **Blood from 264 pediatric cochlear implant users was analyzed for mutations in the *GJB2* gene. Thirty-six aspects of the temporal bone on CT imaging were evaluated in 53 individuals (106 ears) with biallelic disease causing *GJB2* mutations. A subset of patients was age matched and compared with normally hearing individuals. Subjects with biallelic *GJB2* mutations were tested for mutations in the *SLC26A4* gene to rule out Pendred syndrome as a confounding cause of large vestibular aqueduct syndrome.** ***Results:*** **Approximately 53% of ears of subjects (72% of subjects) with biallelic *GJB2* mutations had at least one temporal bone anomaly. The most common findings were 1) dilated endolymphatic fossa (28%); 2) hypoplastic modiolus (25%); 3) large vestibular aqueduct (8%); 4) hypoplastic horizontal semicircular canal (8%); 5) hypoplastic cochlea (4%). Compared with normally hearing individuals, the *GJB2* group had hypoplasia of the cochlear nerve canal, lateral semicircular canal vestibule, internal auditory canal (*t* tests, $P < .001$), and were 11 times more likely to have a hypoplastic modiolus. Dilated endolymphatic fossae were 1.4 times more common in the *GJB2* group, and large vestibular aqueducts were 3 times more common in the *GJB2* group, as compared with normally hearing controls.** ***Conclusions:*** **Temporal bone anomalies are common in *GJB2*-related HL, and imaging of the temporal bone should be included in routine evaluation of these individuals.** ***Key Words:*** **Temporal bone, tomography, CT, *GJB2*, connexins, measure, Pendred, *SLC26A4*.**

Laryngoscope, **116:2178–2186, 2006**

INTRODUCTION

Mutations in the *GJB2* gene (connexin 26) are believed to be associated with bilateral sensorineural hearing loss (SNHL) without temporal bone computed tomography (CT) anomalies.[1–4] Consequently, one paradigm for investigating childhood idiopathic SNHL recommends against imaging the temporal bone in children with biallelic *GJB2* mutations.[5] The objective of this study was to see whether a battery of measures from CT imaging could identify temporal bone anomalies in individuals with *GJB2*-related HL. Identification of such anomalies would support the routine use of imaging in *GJB2*-related HL and would suggest that paradigms for investigating SNHL be revised to incorporate this investigation.

Autosomal recessive nonsyndromic HL is the most prevalent genetic cause of congenital HL, and 50% of profound cases are caused by mutations in the *GJB2* gene.[4] The *GJB2* gene encodes the connexin 26 (Cx26) protein, which is a component of gap junctions. Gap junctions in the cochlea allow potassium ions to be removed from endolymph to the stria vascularis to maintain endolymphatic homeostasis.[6] Mutations in Cx26 are presumed to result in altered potassium recirculation, leading to accumulation of potassium in the cochlear endolymph and causing hair cell dysfunction and deafness.[7] The phenotype profile of *GJB2*-related HL is heterogeneous and depends on the severity of the *GJB2* mutation and its protein product.[4] More than 100 Cx26 mutations known to cause SNHL have been reported in 35 different countries.[8]

The few small studies investigating temporal bone imaging in *GJB2* deafness relied on visual inspection and did not find a reliable association between *GJB2* mutations and temporal bone anomalies. Kenna et al.[9] investigated 18 children with biallelic *GJB2* mutations and found one individual with asymmetry of the right modiolus. Preciado et al.[5] studied 21 children with biallelic *GJB2* mutations and identified one borderline large vestibular aqueduct (LVA). Normal temporal bone CT imaging has been reported in separate groups of 19 and 23 individuals with biallelic *GJB2* mutations.[2,3] Green et al.[4] reported no cochlear abnormalities in any individuals referred for HL or cochlear implantation.

From the Department of Otolaryngology–Head and Neck Surgery (E.J.P., R.V.H., K.A.G., B.C.P.), the Division of Neuroradiology (S.B.), and the Molecular Genetics Laboratory, Department of Paediatric Laboratory Medicine (T.L.S.), The Hospital for Sick Children, Toronto, Canada.

Editor's Note: This Manuscript was accepted for publication August 24, 2006.

This research was supported by the Chapnik, Freeman and Friedberg Clinician Scientist Fund, the Judy Chauvin Otolaryngology Resident Award, and the Masonic Foundation of Ontario.

Send correspondence to Dr. Evan J. Propst, Cochlear Implant Program, Department of Otolaryngology–Head and Neck Surgery, 6th Floor, Elm Wing, The Hospital for Sick Children, 555 University Avenue, Toronto, Ontario, M5G 1X8, Canada. E-mail: evan.propst@utoronto.ca

DOI: 10.1097/01.mlg.0000244389.68568.a7

We recently demonstrated in children with syndromic HL that visual inspection combined with precise measurement of the temporal bone on CT imaging can detect many more anomalies than with visual inspection alone.[10] On the basis of this premise, the purpose of the present study was to describe temporal bone findings using visual inspection and direct measurement of CT imaging in individuals with *GJB2*-related HL. We asked whether evaluation of the temporal bone is required in individuals with biallelic *GJB2* mutations.

MATERIALS AND METHODS

Subjects

Subjects were pediatric cochlear implant users with bilateral severe to profound SNHL. This project was approved by The Hospital for Sick Children Ethics Review Board. Blood was prospectively obtained from 264 nonsyndromic patients with nonprogressive SNHL after obtaining written consent from each child's parent/guardian. Patients with disease-causing biallelic *GJB2* mutations were included. Normally hearing controls were sequential trauma patients with petrous CT studies identified by way of a radiology report text search program using keywords "petrous" and "trauma." A chart review yielded 32 individuals with CT imaging of the temporal bone who were nonsyndromic and who had a normal audiogram.

DNA Extraction and Mutation Analysis

DNA was extracted from whole blood using high salt (Gentra Systems, Inc, Minneapolis, MN) or spin column (Qiagen Inc., Valencia, CA) methods. Extracted DNA was stored in TE buffer (10 mmol/L Tris-HCl, 1 mmol/L EDTA pH 8.0). Mutation detection for the GJB2 gene was performed by direct sequencing of the coding region (exon 2) and the intron/exon boundaries. This process has been described in detail elsewhere.[11] Samples were sequenced in both directions.

Several patients with *GJB2*-related HL had a LVA, and therefore all patients with biallelic *GJB2* mutations were tested for mutations in the *SLC26A4* gene that is associated with Pendred syndrome and LVA. Mutation detection for the *SLC26A4* gene was performed by direct bidirectional sequencing of the coding region and intron/exon boundaries of the gene (primers available on request). Polymerase chain reaction (PCR) reactions contained in a 50 uL volume 100 ng genomic DNA, 40 pmol each forward and reverse primer, 1.5 mmol buffer (1.5 mmol MgCl2, 500 mmol KCl, 100 mmol Tris-HCl, pH8.8), 200 μmol each dNTP (Amersham Biosciences/GE Health Care, Piscataway, NJ), and 1.5 U *Taq* polymerase (Amplitaq Gold, Roche Molecular Systems, Pleasanton, CA). PCR conditions used were initial denaturation of 95°C 10 minutes; touchdown step cycle (15 cycles) 95°C for 30 seconds, 65.5°C to 58°C for 30 seconds decreasing 0.5°C per cycle, 72°C for 30 seconds; cycle (20 cycles) 95°C for 30 seconds, 58°C for 30 seconds, 72°C for 30 seconds; and final extension of 72°C for 2 minutes. Sequencing reactions were performed as described for *GJB2* mutation detection.

Temporal Bone Evaluation

Temporal bone CT imaging previously obtained for clinical reasons was evaluated. Similar digitally stored CT imaging was available for *GJB2* and control groups, which were randomized and displayed to a blinded neuroradiologist using the Centricity Picture Archiving Communication System (PACS) by General Electric. Items evaluated on each CT image appear in Table I. Precise measurements (recorded in millimeters and rounded to 2 decimal points) were made using electronic calipers provided by the PACS system. Immeasurable aspects of the temporal bone were categorized by visual inspection. Thirty-six aspects of each temporal bone were evaluated using CT imaging: 16 by direct measurement, 12 computed from direct measurement, and 8 by visual inspection. Thirty-three recordings from each ear were made on axial section, and three were made on coronal section.

Statistical Analysis

We report first temporal bone findings of all individuals with biallelic disease causing *GJB2* mutations. Because certain temporal bone structures grow with age, we then compared a subset of the *GJB2* group with age-matched controls. Measurements across groups were compared using *t* tests for continuous variables and Mann-Whitney tests for categorical data. Significance was defined as $P \leq .001$ after Bonferroni correction, which was used to raise the standard of proof when making multiple comparisons across temporal bones. Statistics reflect the number of ears evaluated. Because several criteria exist for diagnosing a large endolymphatic fossa (opening into aqueduct) and a dilated endolymphatic duct, we calculated positive and negative predictive values (PPV and NPV, respectively) to assess the probability that each of these criteria in isolation could predict the presence or absence of biallelic *GJB2* mutations.

RESULTS

GJB2 Mutation Detection

Blood from 264 nonsyndromic pediatric cochlear implant users was analyzed for *GJB2* mutations. Biallelic *GJB2* mutations were identified in 56 (21%) patients. Eleven different disease causing *GJB2* mutations were identified (Table II).[8,11,12] The G109A(V37I) mutation has been described as a benign polymorphism and a disease causing mutation, and therefore, three subjects with this mutation were omitted from analysis.[11,12]

SLC26A4 Mutation Detection

Blood from 53 subjects with biallelic *GJB2* mutations was analyzed for mutations in the *SLC26A4* gene (Pendred syndrome). None had homozygous *SLC26A4* mutations. Four patients with biallelic *GJB2* mutations were heterozygous for sequence changes in the *SLC26A4* gene. One patient with the *GJB2* genotype 35delG/35delG was heterozygous for a nonsense mutation T1790G (L597×), which is likely disease causing.[13] Three additional patients were heterozygous for novel *SLC26A4* sequence changes of unknown significance: one was heterozygous for C296T (T99M) (*GJB2* genotype 35delG/167delT), another was heterozygous for an intronic change C1544 + 9T (*GJB2* genotype 35delG/35delG), and a third was heterozygous for C1488T (L496L) (*GJB2* genotype 35delG/T107C).[13]

Temporal Bone Evaluation

Temporal bone CT imaging of 53 patients (106 ears) with biallelic disease-causing *GJB2* mutations was reviewed. Subjects were 33 males, 20 females, with a mean age of 3.60 ± 3.90 years. Approximately 53% (56/106) of ears had at least one temporal bone anomaly by judgment or measurement criteria. Approximately 72% (38/53) of subjects had at least one temporal bone anomaly, and 47% (18/38) of these subjects had bilateral anomalies. The most common findings were 1) dilated endolymphatic fossa (28.3% by judgment, 26.4% measuring greater than 2 mm, 29.2% by either

TABLE I.
Summary of Computed Tomography Measurements Obtained in Axial and Coronal Planes.

Structure	Description of Measurement
Inner ear	
Cochlea apical turn hypoplastic?	On cut of cochlea demonstrating modiolus and eighth nerve canal, judgment if apical turn of cochlea is smaller than expected
Cochlea apical turn AP	On same cut, measurement of AP diameter of apical turn
Cochlea apical turn transverse	On same cut, measurement of transverse diameter of apical turn
Cochlea apical turn ratio AP:transverse	Calculated ratio of AP to transverse dimensions of apical turn
Cochlea basal turn AP	On cut of cochlea demonstrating basal turn, measurement of AP diameter
Cochlea basal turn transverse	On same cut, measurement of transverse diameter
Cochlea basal turn ratio AP:transverse	Calculated ratio of AP to transverse dimensions of basal turn
Modiolus shape	On cut of apical turn of cochlea, judgment if modiolus is normal shape (square), tall, "c"-shaped, or absent
Modiolus dimension AP	On same cut, measurement of AP diameter of modiolus
Modiolus dimension transverse	On same cut, measurement of transverse diameter of modiolus
Modiolus ratio AP:transverse	Calculated ratio of AP to transverse dimensions of modiolus
Cochlear nerve canal width	On same cut, measurement between bony edges of eighth nerve canal
Horizonal semicircular canal	
Hypoplastic?	Judgment if canal is of normal size or smaller than expected
Bony island width	Measurement of bony island in dimension perpendicular to long axis of vestibule
Vestibule width	Measurement of vestibule in dimension perpendicular to long axis of vestibule
Vestibule length	Measurement of long axis of vestibule
Vestibule ratio width:length	Calculated ratio of vestibule width to length
Ampulla dilated?	Judgment if ampulla is normal size or dilated
Posterior semicircular canal	
Canal diameter	Measurement of diameter of posterior semicircular canal lumen
Endolymphatic fossa	
Fossa enlarged? (judgment)	Judgment if opening into vestibular aqueduct is enlarged
Fossa size	Measurement of opening into vestibular aqueduct
Fossa larger than 2 mm?	Judgment if fossa is large defined as measurement greater than 2 mm
Vestibular aqueduct	
Aqueduct enlarged? (judgment)	Judgment if vestibular aqueduct width midway between fossa and horizontal SCC is larger than width of posterior semicircular canal
Aqueduct size	Measurement of aqueduct midway between fossa and horizontal SCC
Aqueduct larger than 1.5 mm?	Judgment if aqueduct is large defined as measurement greater than 1.5 mm
Aqueduct larger than posterior SCC?	Judgment if measurement of aqueduct is larger than measurement posterior SCC
Magnitude of enlargement	Judgment if aqueduct is normal, large, or extra large compared with posterior semicircular canal
Shape	Judgment if walls of aqueduct are funnel-shaped or parallel to each other
IAC	
IAC length	On same cut, measurement from the lamina cribrosa to a line drawn across the opening of the porous acousticus
Porous acousticus width	On same cut, measurement across opening of the porous acousticus
IAC ratio porous width:length	Calculated ratio of porous width to IAC length
IAC mid-distance width	On same cut, measurement of the IAC width at a distance midway along the length of the IAC
IAC ratio mid-distance:porous width	Calculated ratio of IAC mid-distance width to porous width
Porous acousticus height (coronal)	On coronal section, height of opening of porous acousticus
IAC length (coronal)	On coronal section, length from porous acousticus to lamina cribrosa
IAC ratio porous:length (coronal)	Calculated ratio of porous width (coronal) to IAC length (coronal)

AP = anteroposterior; SCC = semicircular canal; IAC = internal auditory canal.

judgment or measurement criteria) (Fig. 1); 2) modiolar deficiency (24.7% abnormal: 19% tall and narrow, 3.8% "c"-shaped, 1.9% absent) (Fig. 2); 3) LVA (14.2% by judgment, 7.5% measuring greater than the posterior semicircular canal, 1.9% measuring greater than 1.5 mm, 15.7% by either judgment or measurement criteria) (Fig. 3); 4) hypoplastic horizontal semicircular canal (7.5%) (Fig. 4); 5) hypoplastic cochlea (3.8%) (Fig. 2); 6) dilated ampulla (3.8%). Other

TABLE II.
Biallelic *GJB2* Mutations.

Mutation Name	Number of Individuals (Total, n = 56)	Mutation Type	Effect on Protein
35delG/35delG	38	Deletion,frameshift/deletion,frameshift	Truncating/truncating
35delG/167delT	5	Deletion,frameshift/deletion,frameshift	Truncating/truncating
167delT/167delT	1	Deletion,frameshift/deletion,frameshift	Truncating/truncating
35delG/235delC	1	Deletion,frameshift/deletion,frameshift	Truncating/truncating
235delC/235delC	1	Deletion,frameshift/deletion,frameshift	Truncating/truncating
35delG/T107C (L36P)	1	Deletion,frameshift/missense	Truncating/nontruncating
35delG/T229C (W77R)	1	Deletion,frameshift/missense	Truncating/nontruncating
35delG/C298T (H100Y)	1	Deletion,frameshift/missense	Truncating/nontruncating
35delG/G551C (R184P)	1	Deletion,frameshift/missense	Truncating/nontruncating
35delG/G109A(V37I)	1	Deletion,frameshift/missense	Truncating/nontruncating
G109A(V37I)/G109A(V37I)	2	Missense/missense	Truncating/nontruncating
G71A(W24×)/G71A(W24×)	1	Nonsense/nonsense	Truncating/truncating
G71A(W24×)/407dupA	1	Nonsense/insertion,frameshift	Truncating/truncating
35delG/269insT	1	Deletion,frameshift/insertion,frameshift	Truncating/truncating

abnormalities included four dehiscent posterior semicircular canals (Fig. 5), two dehiscent superior semicircular canals, one pericochlear lucency, and one vestibular aqueduct extending into the ampulla. LVAs were more commonly large (93.3%) than extra large (6.7%) and more often had parallel (73.3%) rather than funnel shaped (26.7%) walls.[14]

Within the *GJB2* group, compound heterozygotes had 1.5 times more temporal bone anomalies than homozygotes (75% vs. 46%, respectively). Similarly, individuals with mutations other than homozygous 35delG had 1.4 times more temporal bone anomalies and were more likely to have an LVA by visual inspection, as compared with 35delG homozygotes (67% vs. 47%, respectively; Mann-Whitney, $P \leq .001$). Individuals with two truncating *GJB2* mutations had a significantly shorter internal auditory canal length (*t* test, $P \leq .001$) and a 2% to 15% prevalence of LVA (depending on diagnostic criteria used, i.e., judgment, larger than 1.5 mm, larger than posterior semicircular canal) as compared with subjects possessing both truncating and nontruncating mutations (0% prevalence of LVA).

A subset of 21 patients (42 ears) from the *GJB2* group were age matched and compared with 21 normally hearing controls (42 ears). Table III illustrates temporal bone measurements for both groups. Temporal bone anomalies were detected in 55% of the *GJB2* group and 29% of controls. Subjects in the *GJB2* group had a significantly smaller cochlear nerve canal width (Fig. 6) and were 11 times more likely to have an abnormally shaped modiolus (27% tall and narrow, 5% "c"-shaped, 5% absent) as compared with controls (3% "c"-shaped) (Mann-Whitney, $P \leq .001$) (Fig. 2). There was a trend for the *GJB2* group to have smaller apical and basal turns of the cochlea (*t* test, $P > .001$) (Fig. 2). The horizontal semicircular canal vestibule width-to-length ratio was significantly smaller in the *GJB2* group, denoting that the vestibule is longer and narrower as compared with controls (Fig. 4). There was a trend for the posterior semicircular canal to be smaller in the *GJB2* group (*t* test, $P > .001$).

Approximately 33% of the *GJB2* group and 25% of the control group had an enlarged endolymphatic fossa

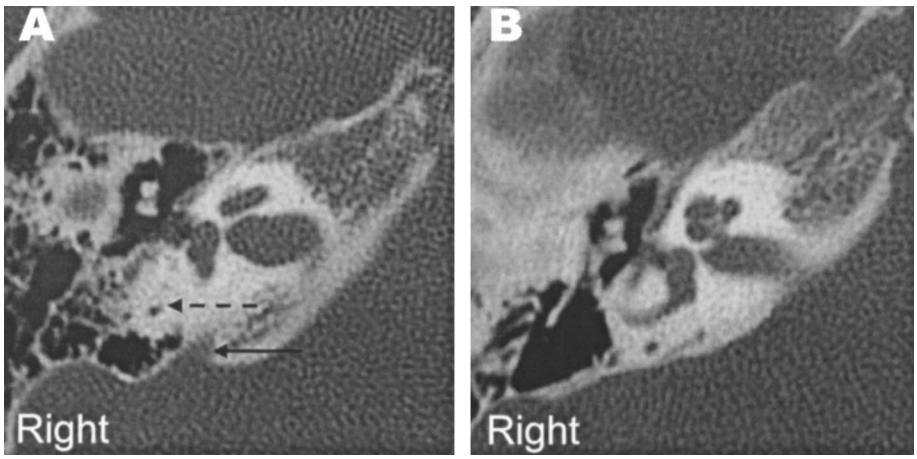

Fig. 1. Endolymphatic fossa, axial section. Note large, funnel-shaped endolymphatic fossa (black arrow) that is larger than posterior limb of posterior semicircular canal (dashed black arrow) in a child with *GJB2* mutation 35delG/167delT (A) as compared with normally hearing control (B).

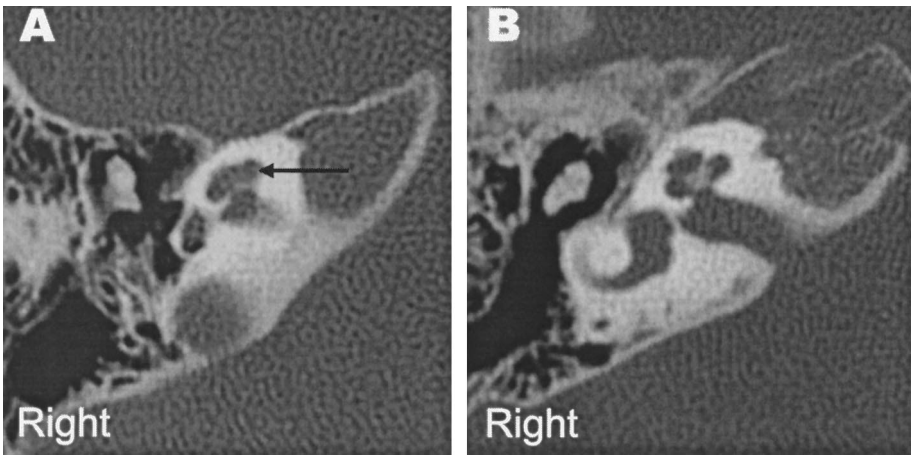

Fig. 2. Cochlea, axial section. Note hypoplastic cochlea (black arrow) that is lacking central bony modiolus in a child with *GJB2* mutation 35delG/35delG (A) as compared with normally hearing control (B).

(Fig. 1). Fossae in the *GJB2* group were 1.4 times more likely to be evaluated as enlarged on the basis of visual inspection or measurement greater than 2.0 mm. The neuroradiologist's judgment based on visual inspection was as accurate as using measurement criteria. There was a trend for the width of the endolymphatic fossa to be larger in the *GJB2* group as compared with controls (*t* test, $P > .001$). The probability that a person with an enlarged fossa (greater than 2 mm) had *GJB2*-related HL (PPV) was 64%, and the probability that a person with a fossa smaller than 2 mm had normal hearing (NPV) was 54%.

An LVA was evident in 17% of the *GJB2* group and 5% of controls by judgment criteria (Fig. 3). The mean aqueduct diameter in the *GJB2* group was 1.5 times larger than in controls. There was a trend toward a greater incidence of LVA in the *GJB2* group using measurement criteria (Mann-Whitney, $P > .001$). When enlarged, aqueducts in the *GJB2* group were more likely to have parallel walls rather than a funnel-shaped appearance.[14] When the LVA was defined as measuring greater than 1.5 mm, the sensitivity was 2%, specificity 100%, PPV 100%, and NPV 50%. When defined as measuring greater than the posterior semicircular canal, the sensitivity was 7%, specificity 100%, PPV 100%, and NPV 51%.

The internal auditory canal in the *GJB2* group had a significantly smaller porous acousticus width (*t* test, $P \leq .001$) and a smaller mid-distance width (*t* test, $P > .001$) as compared with normally hearing controls (Fig. 7). There was no difference in length of the internal auditory canal across groups.

DISCUSSION

GJB2 Mutation Detection. Biallelic *GJB2* mutations were identified in 56 of 264 (21%) cochlear implant users. The most commonly identified *GJB2* mutation was 35delG, which is the most common *GJB2* mutation worldwide.[8] We omitted subjects with the G109A(V37I) mutation because it has been reported as both a benign polymorphism and a disease-causing mutation, and its function may depend on the cultural background of the individual.[11,12]

SLC26A4 Mutation Detection. Four children were heterozygous (carriers) for novel *SLC26A4* gene changes (1 nonsense mutation, 3 changes of unknown significance) and were considered to have *GJB2*-related HL (2 disease-causing *GJB2* mutations). Because all four *SLC26A4* gene changes were heterozygous, they are not thought to be contributing to the phenotype seen in these patients. However, this finding reinforces the fact that individuals may inherit changes in several deafness related genes, complicating the analysis of a genetic etiology for their SNHL.

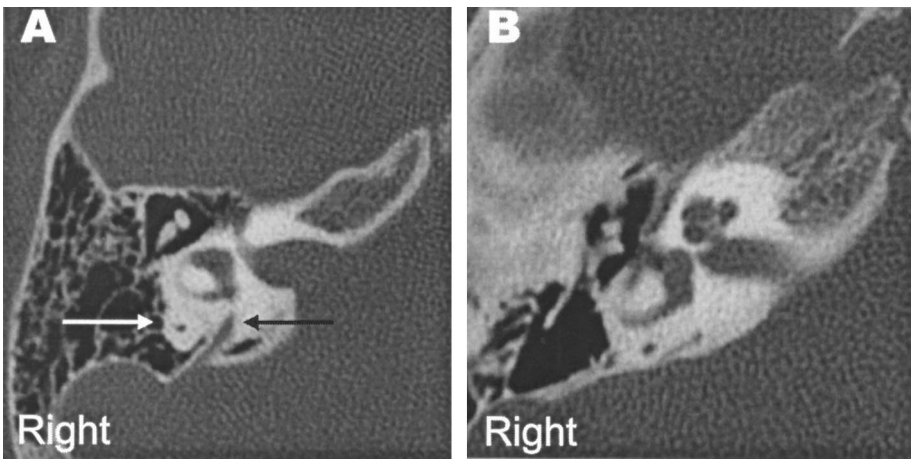

Fig. 3. Vestibular aqueduct, axial section. Note large vestibular aqueduct (black arrow) that is larger than posterior limb of posterior semicircular canal (white arrow) in a child with *GJB2* mutation 35delG/167delT (A) as compared with normally hearing control (B).

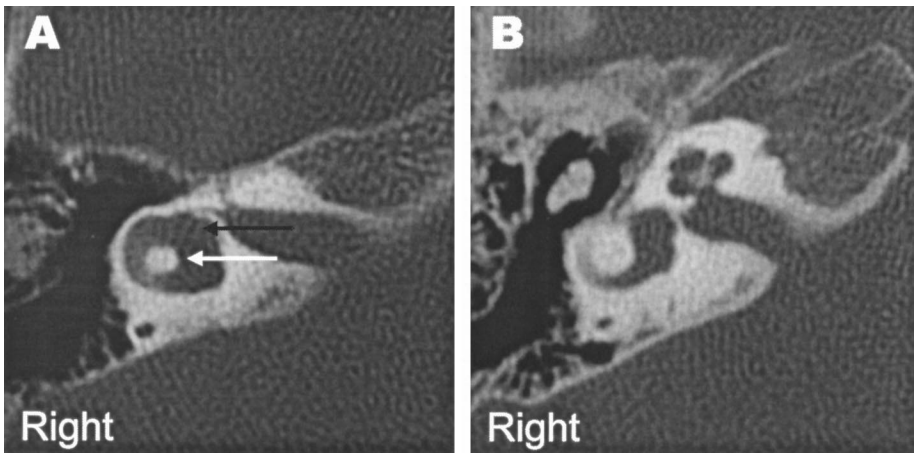

Fig. 4. Horizontal semicircular canal, axial section. Note hypoplastic bony island (white arrow) and long, narrow vestibule (black arrow) in a child with *GJB2* mutation 35delG/35delG (A) as compared with normally hearing control (B).

Temporal Bone Evaluation

Greater than 50% of ears in the *GJB2* group had temporal bone anomalies on CT imaging. The most common findings were dilated endolymphatic fossa, modiolar deficiency, and LVA (Figs. 1 to 3). This is not surprising given that Kenna et al.[9] described one child with a modiolar anomaly, and Preciado et al.[5] identified a child with a borderline LVA.

Within the *GJB2* group, individuals with compound heterozygous mutations, mutations other than homozygous 35delG, and two truncating mutations, were more likely to have temporal bone anomalies as compared with homozygotes, biallelic 35delG mutations, and at least one nontruncating mutation, respectively. This suggests that mutation severity and the ability to produce a functional protein affects the degree of temporal bone irregularity.

A subset of children from the *GJB2* group were age matched with normally hearing controls because certain aspects of the temporal bone grow with age. Temporal bone anomalies were detected almost twice as often in the *GJB2* group as compared with controls (55% vs. 29%, respectively). This suggests that even though normally hearing individuals can have irregular temporal bones, irregularities are more common in *GJB2* deafness.

In the inner ear, the *GJB2* group had a smaller cochlear nerve canal, abnormally shaped modiolus, hypoplastic horizontal semicircular canal vestibule (Fig. 4), and showed a trend toward a hypoplastic cochlea (Figs. 2 and 6). These results are consistent with previous findings of decreased evoked responses of the auditory nerve in *GJB2* deafness, which likely resulted from a decreased number of spiral ganglion neurons.[11] Modiolar deficiency has been associated with endolymphatic gusher during stapes surgery or cochlear implantation.[15] Embryologically, labyrinthine development occurs between 3 and 8 weeks of gestation.[16] Vestibulocochlear hypoplasia in *GJB2* deafness provides evidence for disruption of this process.

A dilated endolymphatic fossa was seen in one third of the *GJB2* group and one quarter of controls, regardless of whether judgment or measurement criteria were used (Fig. 1). A dilated fossa has been associated with vertigo, which may result from conduction of intracranial pressure changes into the vestibule through the aqueduct.[15] In this study, the probability that a person with a fossa larger than 2 mm had *GJB2* deafness (PPV) was 64%, and the probability that a subject with a fossa smaller than 2 mm had normal hearing (NPV) was 54%. This suggests that using a cutoff of 2 mm should not be used in isolation to diagnose *GJB2* related SNHL but may be helpful as an adjunctive measure.

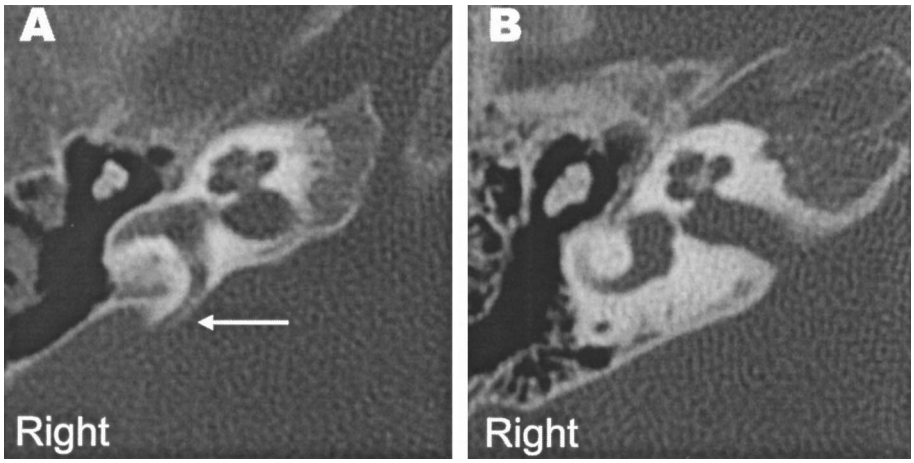

Fig. 5. Horizontal semicircular canal, axial section. Note dehiscent posterior aspect of horizontal semicircular canal (white arrow) in a child with *GJB2* mutation 35delG/35delG (A) as compared with normally hearing control (B).

TABLE III.
Summary of Computed Tomography Measurements, Calculated Ratios, and Categorical Evaluations for Age-Matched Subset of Subjects.

Structure	*GJB2*			Control			Difference *P* Value
	n (ears)	Mean/%	SD	n (ears)	Mean/%	SD	
Inner ear							
Cochlea apical turn hypoplastic?	42	5%		42	0%		.155
Cochlea apical turn AP	42	3.11	0.42	42	3.23	0.35	.189
Cochlea apical turn transverse	42	5.76	0.45	42	5.93	0.25	.031
Cochlea apical turn ratio AP:transverse	42	0.54	0.07	42	0.54	0.06	.849
Cochlea basal turn AP	42	2.24	0.23	42	2.33	0.25	.106
Cochlea basal turn transverse	42	8.86	0.52	42	9.07	0.50	.057
Cochlea basal turn ratio AP:transverse	42	0.25	0.03	42	0.26	0.03	.648
Modiolus shape	41	37% abnormal		39	3% abnormal		.000*
Modiolus dimension AP	39	1.52	0.23	40	1.39	0.17	.004
Modiolus dimension transverse	39	1.82	0.45	40	1.86	0.36	.636
Modiolus ratio AP:transverse	39	0.92	0.37	40	0.80	0.30	.118
Cochlear nerve canal width	42	2.04	0.24	41	2.25	0.32	.001*
Horizontal semicircular canal							
Hypoplastic?	42	2%		42	5%		.559
Bony island width	42	3.96	0.44	42	3.83	0.48	.214
Vestibule width	42	2.98	0.33	42	3.13	0.24	.024
Vestibule length	42	6.05	0.43	42	5.90	0.33	.072
Vestibule ratio width:length	42	0.49	0.05	42	0.53	0.04	.000*
Ampulla dilated?	42	0%		42	0%		1.00
Posterior SCC	42	0.98	0.17	42	1.09	0.18	.010
Endolymphatic fossa							
Fossa enlarged? (judgment)	42	33%		41	24%		.372
Fossa size	42	1.49	1.10	41	1.25	0.90	.280
Fossa larger than 2 mm?	42	33%		41	20%		.156
Vestibular aqueduct							
Aqueduct enlarged? (judgment)	42	17%		41	5%		.086
Aqueduct size	42	0.56	0.34	41	0.38	0.32	.018
Aqueduct larger than 1.5 mm	42	2%		41	0%		.323
Aqueduct larger than posterior SCC	42	7%		41	0%		.083
Magnitude of enlargement	14	86% large		2	100% large		.593
Shape	14	86% parallel		2	50% parallel		.312
IAC							
IAC length	42	9.10	1.97	42	9.06	1.92	.929
Porous acousticus width	42	5.94	1.01	42	6.76	1.08	.001*
IAC ratio porous width:length	42	0.68	0.18	42	0.77	0.17	.022
IAC mid-distance width	42	4.91	1.02	42	5.34	0.95	.049
IAC ratio mid-distance:porous width	42	0.84	0.17	42	0.81	0.20	.538
Porous acousticus height (coronal)	42	4.67	0.96	33	5.06	0.74	.061
IAC length (coronal)	41	10.81	2.13	33	10.98	2.09	.736
IAC ratio porous:length (coronal)	41	0.45	0.13	33	0.48	0.10	.334
Overall evaluation							
Any abnormality judgment or measure	42	55%		42	29%		.016
Any large fossa by measurement criteria	42	33%		41	20%		.156
Any large fossa judge or measure	42	36%		41	24%		.264
Any large aqueduct by measurement criteria	42	7%		41	0%		.083
Any large aqueduct judge or measure	42	7%		41	0%		.083
Any large fossa or aqueduct by measurement	42	33%		41	20%		.156
Any large fossa or aqueduct judge or measure	42	36%		41	24%		.264

*$P < .001$ after Bonferroni correction.
AP = anteroposterior; SCC = semicircular canal; IAC = internal auditory canal.

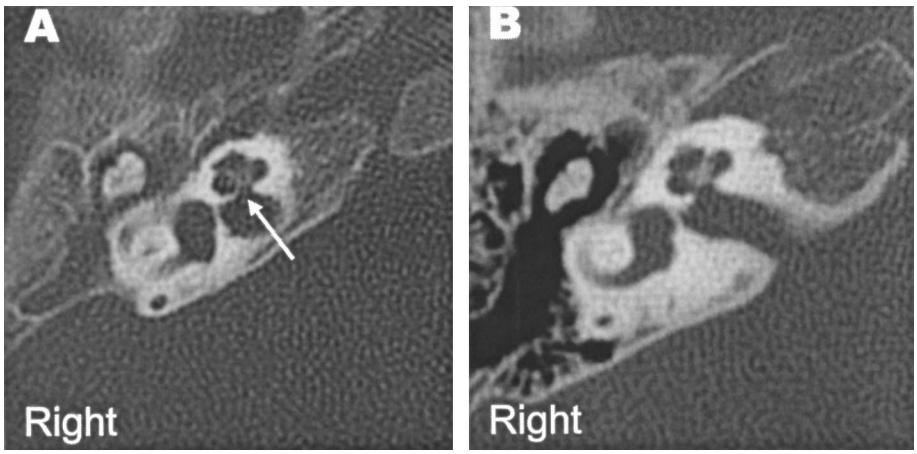

Fig. 6. Cochlea, axial section. Note narrow cochlear nerve canal (white arrow) in a child with *GJB2* mutation 35delG/35delG (A) as compared with normally hearing control (B).

An LVA by visual inspection and measurement was three times more common in the *GJB2* group as compared with controls (Fig. 3). Interestingly, LVA was diagnosed by visual inspection only half as frequently as an enlarged fossa, and the number of LVAs decreased when measurement criteria were used (greater than 1.5 mm or greater than posterior semicircular canal). Defining the LVA as measuring greater than 1.5 mm attained a sensitivity of 2%, specificity 100%, PPV 100%, and NPV 50%, suggesting a high likelihood of association with *GJB2* deafness, but suggests that using this criteria alone would miss the diagnosis in most people. Similarly, defining the LVA as measuring greater than the posterior semicircular canal attained sensitivity of 7%, specificity 100%, PPV 100%, and NPV 51%.

The internal auditory canal in the *GJB2* group had a smaller porous width with a normal length, suggesting the canal is long and narrow compared with controls (Fig. 7). During embryogenesis, the otic vesicle produces a growth factor that promotes survival of the vestibulocochlear nerve, which inhibits cartilage formation leading to formation of the internal auditory canal.[17] In *GJB2*-related HL, the hypoplastic labyrinth and modiolus may lead to underdevelopment of the vestibulocochlear nerve, which cannot maximally inhibit cartilage formation, resulting in a narrow internal auditory canal.

Implications

Results from this study have important implications on our understanding of the mechanism of *GJB2* deafness. *GJB2* deafness is presumed to result from irregular endolymphatic homeostasis.[6,7] However, this study found a relation between *GJB2* mutations and temporal bone anomalies. This suggests that either *GJB2* mutations independently affect gap junction and bony labyrinthine development or that *GJB2* mutations disrupt gap junctions and endolymphatic homeostasis, which then leads to irregular bony labyrinthine development.

Clinically, anomalous cochleovestibular anatomy has been associated with difficulty during and after cochlear implantation. In a large review at our institution of children with cochleovestibular anomalies, 17.5% had middle ear abnormalities, making it difficult to access the cochlea, 14% had a facial nerve with an aberrant course, precluding optimal cochleostomy placement, and 6.7% had perilymph leak at implantation.[14] Children with narrow cochlear nerve or internal auditory canals performed more poorly on tests of speech perception, and the author suggested they could be considered poorer candidates for implantation.[14] This is supported by our previous finding of decreased auditory nerve evoked responses in individuals with *GJB2* deafness.[11] Results from the present study suggest that evaluation of the temporal bone in *GJB2*

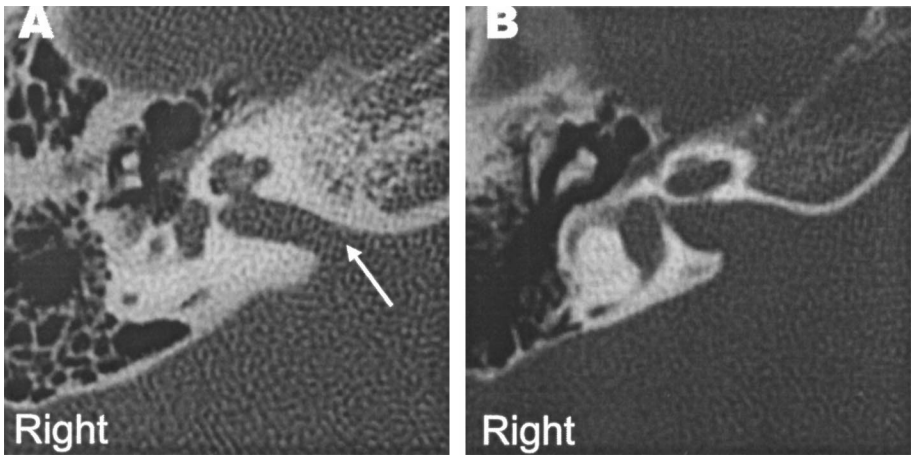

Fig. 7. Internal auditory canal, axial section. Note long and narrow internal auditory canal with small porous acousticus (white arrow) in a child with *GJB2* mutation W24×/W24× (A) as compared with normally hearing control (B).

related HL is necessary before implantation because of the information that may be gleaned from potentially identifying anomalous cochleovestibular anatomy.

CONCLUSION

Detailed evaluation of temporal bone imaging identified anomalies in over 50% of ears (72% of individuals) with *GJB2*-related HL. The most commonly identified abnormalities were 1) dilated endolymphatic fossa; 2) hypoplastic modiolus; 3) LVA; 4) hypoplastic semicircular canal; 5) hypoplastic cochlea. *GJB2* deafness was also associated with a hypoplastic cochlear nerve canal and a narrow internal auditory canal. These anomalies may be associated with difficulties during and after cochlear implantation. Results suggest that imaging of the temporal bone should be performed in individuals with *GJB2*-related HL and that previously described diagnostic algorithms for investigating childhood SNHL should be revised to incorporate this important investigation.

Acknowledgments

The authors thank the families described in this study for their support. The authors are indebted to Richard Mount, Patt Fuller, the audiologists, speech and language pathologists, and secretarial staff in the Department of Otolaryngology, Leslie Steele and the staff in the Department of Molecular Genetics, and the nurses and anesthetists of N OR for their assistance.

BIBLIOGRAPHY

1. Norton SJ, Perkins JA. Early detection and diagnosis of infant hearing impairment. In: Cummings CW, Flint PW, Harker LA et al, eds. *Cummings Otolaryngology Head & Neck Surgery*, 4th ed. Philadelphia: Elsevier Moseby, 2005:4392.
2. Cohn ES, Kelley PM, Fowler TW, et al. Clinical studies of families with hearing loss attributable to mutations in the connexin 26 gene (*GJB2*/DFNB1). *Pediatrics* 1999;103: 546–550.
3. Denoyelle F, Marlin S, Weil D, et al. Clinical features of the prevalent form of childhood deafness, DFNB1, due to a connexin-26 gene defect: implications for genetic counseling. *Lancet* 1999;353:1298–1303.
4. Green GE, Mueller RF, Cohn ES, et al. Audiological manifestations and features of connexin 26 deafness. *Audiol Med* 2003;1:5–11.
5. Preciado DA, Lim LHY, Cohen AP, et al. A diagnostic paradigm for childhood idiopathic sensorineural hearing loss. *Otolaryngol Head Neck Surg* 2004;131:804–809.
6. Kikuchi T, Kimura RS, Paul DL, Adams JC. Gap junctions in the rat cochlea: immunohistochemical analysis. *Anat Embryol* 1995;191:101–118.
7. Lefebvre PP, Weber T, Rigo JM, et al. Potassium-induced release of an endogenous toxic activity for outer hair cells and auditory neurons in the cochlea: a new pathophysiological mechanism in Ménière's disease? *Hear Res* 1990;47: 83–93.
8. Propst EJ, Stockley TL, Gordon KA, et al. Ethnicity and mutations in *GJB2* (connexin 26) and *GJB6* (connexin 30) in a multi-cultural Canadian paediatric cochlear implant program. *Int J Pediatr Otorhinolaryngol* 2006;70:435–444.
9. Kenna MA, Wu BL, Cotanche DA, et al. Connexin 26 studies in patients with sensorineural hearing loss. *Arch Otolaryngol Head Neck Surg* 2001;127 1037–1042.
10. Propst EJ, Blaser S, Gordon KA, et al. Temporal bone findings on computed tomography imaging in branchio-otorenal syndrome. *Laryngoscope* 2005;115:1855–1862.
11. Propst EJ, Papsin BC, Stockley TL, et al. Auditory responses in cochlear implant users with and without *GJB2* deafness. *Laryngoscope* 2006;116:317–327.
12. Ballana E, Ventayol M, Rabionet R, et al. Connexins and deafness homepage. Available at: http://www.crg.es/deafness. Accessed June 2006.
13. Chang E, Kolln KA, Nishimura C, et al. Pendred/BOR homepage. Available at: http://www.medicine.uiowa.edu/pendredandbor/. Accessed June 2006.
14. Papsin BC. Cochlear implantation in children with anomalous cochleovestibular anatomy. *Laryngoscope* 2005; 115(1Pt2):1–26.
15. Kronbach GA, van den Boom M, Di Martino E, et al. Computed tomography of the inner ear: size of anatomical structures in the normal temporal bone and in the temporal bone of patients with Ménière's disease. *Eur Radiol* 2005;15:1505–1513.
16. Kenna MA, Hirose K. The ear and related structures, embryology and developmental anatomy of the ear. In: Bluestone CD, Stool SE, Alper CM, et al, eds. *Pediatric Otolaryngology,* vol. 1, 4th ed. Philadelphia: Saunders, 2003: 129–145.
17. Lefebvre PP, Leprince P, Weber T, et al. Neuronotropic effect of developing otic vesicle on cochleo-vestibular neurons: evidence for nerve growth factor involvement. *Brain Res* 1990;22:507:254–260.